Russian Journal of General Chemistry, Vol. 71, No. 6, 2001, pp. 865–872. Translated from Zhurnal Obshchei Khimii, Vol. 71, No. 6, 2001, pp. 921–929.

Emission Properties of the Plasma in Mixtures of Helium with Diethylzinc and Hydrogen Selenide Vapors

A. M. Ob''edkov, G. A. Domrachev, E. Yu. Korovina, and E. N. Razov

Razuvaev Institute of Organometallic Chemistry, Russian Academy of Sciences, Nizhny Novgorod, Russia

Received February 2, 2000

Abstract — The emission properties in the range 200–600 nm of the low-temperature plasma in mixtures of He with Et_2Zn and H_2Se vapors were studied. The spectrum of emission accompanying decomposition of Et_2Zn includes 26 identified lines of Zn atoms and strong emission of electronically excited CH* radicals, and in the case of decomposition of H_2Se two emission lines of Se atoms and an emission band of SeH* radicals are observed. The rate constants of quenching of the levels He 4d $^3D_{2,1}$ and 3*p* $^1P_1$ on introduction into the He plasma of Et_2Zn and H_2Se vapors were determined; Et_2Zn is a stronger quenching agent than H_2Se. Analytical lines allowing monitoring of ZnSe film deposition were selected. Direct plasmochemical decomposition of mixtures of Et_2Zn with H_2Se results in growth of textured ZnSe(cub) layers with substantial inclusions of the hexagonal phase and with carbon-containing inclusions. The photoluminescence spectra of the films obtained exhibit a strong edge band at 460 nm, overlapping with a strong self-activated band centered at 540 nm.

Semiconducting epitaxial films of compositions $A^{III}B^{V}$ and $A^{II}B^{VI}$ provide a basis for modern electronics. Up to now, such materials were mainly prepared by thermal decomposition of volatile organometallic compounds and hydrides of appropriate elements. The results obtained in this field were repeatedly discussed and presented in monographs and reviews (see, e.g., [1–3]). The process for preparing epitaxial films by thermal decomposition under appropriate conditions of volatile organometallic compounds and hydrides was termed the MOCVD process (metalloorganic chemical vapor deposition). Along with the traditional MOCVD process, attempts were made to modify the process for deposition of epitaxial films using, e.g., high-powered lasers and low-temperature plasma. Additional action of plasma on the film deposition process in some cases ensured more efficient decomposition of one or several components and introduction of some dopants; also, for some films the deposition temperature was decreased by 100–200°C as compared to the common MOCVD process. There are numerous reports on successful results obtained in deposition of $A^{III}B^{V}$ and $A^{II}B^{VI}$ epitaxial films by the MOCVD process in combination with additional plasmochemical activation of one or several components. Some examples are presented in Table 1, with the information given on the structure of the forming films, conditions of their preparation, and types of the plasma sources used. As seen from Table 1, most data concern preparation of GaAs, GaN, ZnS, and ZnSe films, as well as ZnS and ZnSe films doped with Mn, Ge, and N. For Group II and III elements, the organometallic precursors were mainly volatile methyl or ethyl derivatives R_nM, and for Group V and VI elements the precursors were hydrides or alkyl derivatives (As, S, Se), or molecular nitrogen. Thus, the set of precursors was typical for the MOCVD process. Plasma was generated by glow, HF, or UHF discharge with varied current and frequency. As plasma-forming gas was mainly used nitrogen or hydrogen. It should be noted that in the majority of studies only one component of reaction mixtures was subjected to plasmochemical activation, e.g., N_2 in deposition of GaN or the component containing dopant in deposition of ZnS:Mn, ZnSe:Ga, and ZnS:N films. In almost all studies the authors' attention was focused mainly on the deposition conditions and composition and properties of the forming films, and no due attention was given to the composition of the plasma in which active species determining the properties of the resulting epitaxial films are generated.

The processes occurring in plasma in mixtures of vapors of organometallic compounds and hydrides with the plasma-forming gas are diverse and complex; therefore, a set of physicochemical methods should be used for studying them. A film deposited on a hot support is formed from species arriving from the gas phase. The burning of plasma is accompanied by intense emission. Therefore, to gain a more complete information on the composition of the gas phase in the course of plasmochemical activation, it is desirable to use such methods as, e.g., emission spectrum analysis,

1070-3632/01/7106-0865 $25.00

Table 1. Conditions for deposition of $A^{III}B^{V}$ and $A^{II}B^{VI}$ films by thermal decomposition of organometallic compounds with plasmochemical activation of separate components

Compound	Reagents, plasma-forming gas	Support	*t*, °C	Plasma source	References
GaAs	Me_3Ga, AsH_3	GaAs	20	Low-frequency glow discharge	[4]
GaAs	Me_3Ga, AsH_3	GaAs	20	Glow discharge	[5]
GaAs	Me_3Ga, $AsH_3(Me_3As)$	GaAs	≤450	"	[6]
GaN	Me_3Ga etherate, N_2	GaAs, Si, GaP, Al_2O_3	150–500	HF discharge of capacitor type	[7]
GaN	Et_3Ga, N_2, H_2	GaAs	500–700	UHF discharge	[8]
GaN	Et_3Ga, N_2, H_2	Al_2O_3	600–700	"	[9]
GaN	Et_3Ga, N_2	Al_2O_3	400–700	HF discharge	[10]
GaN	Et_3Ga, N_2	GaAs	≥20	"	[11]
GaN	Me_3Ga, NH_3	GaAs	550	UHF discharge	[12]
ZnS : Mn	Et_2Zn, H_2S, $MeC_5H_4Mn(CO)_3$	GaAs, GaP	>20	HF discharge	[13]
ZnS	Et_2Zn, H_2S, H_2	Glass	≥170	Glow discharge	[14]
ZnSe	Et_2Zn, Et_2Se_2	GaAs	≥200	"	[15]
$(ZnS)_3(ZnSe)_{42}$	Et_2Zn, Et_2S_2				
ZnSe : Ga	Et_2Zn, Et_3Ga, H_2				
ZnSe : N	Et_2Zn, Et_2Se_2, N_2	ZnSe	350	UHF discharge	[16]
ZnSe, ZnSe : N	Me_2Zn, Et_3N, *t*-Bu_2Se, H_2, N_2	GaAs	315–400	Glow discharge	[17]
ZnSe : N	Me_2Zn, H_2Se, N_2	GaAs	350	"	[18]
ZnSe, ZnSe : N	Me_2Zn, Et_3N, $(t\text{-}Bu)_2Se$	GaAs	315–400	"	[19]

allowing control of the state of the gas phase in the course of deposition of semiconducting films. Yamamoto and Taguchi [16], using emission spectrum analysis, detected and identified active species in the gas phase of UHF discharge in nitrogen: electronically excited atoms N^* and molecules N_2^*. In contrast to [15–19], we performed deposition of semiconducting ZnSe films from Et_2Zn and H_2Se in the electrodeless HF discharge helium plasma, with direct action of plasma on all the components. First, we studied in detail the emission spectra of the electrodeless HF discharge plasma in prepurified helium. The emission spectrum of the electrodeless HF discharge plasma in helium that was not passed thorough the purification system contains, along with strong emission lines of electronically excited helium atoms, also strong emission lines and bands of impurity atoms and molecules. The following lines and bands were detected: emission line of H^* (λ_{em} 486.133 nm), emission bands of N_2^* (second positive system) and N_2^{+*} (first negative system), weak emission band of the electronically excited radicals CH^*, a system at 430.0 nm ($A\ ^2\Delta \rightarrow x\ ^2\prod$ transition), a weak system of the OH^* radical at 306.4 nm, and several emission lines of moderate intensity, originating most probably from electronically excited argon and neon atoms. In the emission spectra of the electrodeless HF discharge plasma in helium after passing the purification system, we detected, along with the very strong emission lines of electronically excited helium atoms, also an emission line of H^* (486.133 nm) and very weak emission lines of N_2^* (second positive system) and N_2^{+*} (first negative system); their intensity was by a factor of 5–6 lower than that observed without purification of helium. The emission bands of OH^* and CH^* and emission lines of argon and neon atoms were not observed. In Table 2 are given the He^* lines observed in the emission spectrum of the electrodeless HF discharge plasma in helium after passing the purification system. The resonance lines corresponding to transitions to the ground $1s\ ^1S_0$ state of the helium atom lie in the vacuum UV range, as well as the intercombination line of helium $2p\ ^3P_{2,1} \rightarrow 1s\ ^1S_0$ (59.1 nm). We could not observe these lines with available equipment. The helium lines were assigned on the basis of reference data [20]. The wavelengths of the emission lines in Table 2 and subsequent tables are given in accordance with the spectral line tables [21]. Table 2 shows that the emission spectra of the electrodeless HF discharge plasma in helium after passing the purification sys-

Table 2. He^* lines observed in the emission spectrum of the electrodeless HF discharge helium plasma

λ_{em}, nm	Assignment	E_{II}, eV[a]
294.511	$2s\ ^3S_1 \longleftarrow 5p\ ^3P_{2,1,0}$	24.03
318.775	$2s\ ^3S_1 \longleftarrow 4p\ ^3P_{2,1,0}$	23.71
370.501	$2p\ ^3P_{2,1} \longleftarrow 7d\ ^3D_{3,2,1}$	24.31
381.961	$2p\ ^3P_{2,1} \longleftarrow 6d\ ^3D_{3,2,1}$	24.21
388.865	$2s\ ^3S3_1 \longleftarrow 3p\ ^3P_{2,1,0}$	23.01
396.473	$2s\ ^1S_0 \longleftarrow 4p\ ^1P_1$	23.74
402.619	$2p\ ^3P_{2,1} \longleftarrow 5d\ ^3D_{3,2,1}$	24.04
412.082	$2p\ ^3P_{2,1} \longleftarrow 5s\ ^3S_1$	23.79
438.793	$2p\ ^1P_1 \longleftarrow 5d\ ^1D_2$	24.04
447.148	$2p\ ^3P_{2,1} \longleftarrow 4d\ ^3D_{3,2,1}$	23.73
471.315	$2p\ ^3P_{2,1} \longleftarrow 4s\ ^3S_1$	23.59
492.193	$2p\ ^1P_1 \longleftarrow 4d\ ^1D_2$	23.74
501.568	$2s\ ^1S_0 \longleftarrow 3p\ ^1P_1$	23.09
507.774	$2p\ ^1P_1 \longleftarrow 4s\ ^1S_0$	23.67
587.562	$2p\ ^3P_{2,1} \longleftarrow 3d\ ^3D_{2,1}$	23.07
587.597	$2p\ ^3P_0 \longleftarrow 3d\ ^3D_1$	23.07

[a] (E_{II}) Energy required for excitation of the upper state of the helium atom from the ground state ($1s\ ^1S_0$).

tem, taken under standard conditions ($P_{He} \cong 82.6 \pm 5.2$ Pa, output power of HF generator ~100 W) contain the emission lines of electronically excited helium atoms whose excitation requires consumption of approximately 23.0–24.2 eV. No emission lines of electronically excited He^+ ions were observed. The most suitable working lines for further experiments in the dynamic mode using an MDR-3 monochromator are the He^* lines at 447.148 and 501.568 nm. These lines are fairly strong, the background in this region is low, and there is no overlap with the other lines.

When introduced into the helium flow in the zone of the electrodeless HF discharge, Et_2Zn molecules decomposed. A zinc-containing film deposited on the GaAs support and on the walls of the plasmochemical reactor, and in the gas phase over the support intense emission of the Et_2Zn decomposition products was observed. Analysis of the emission spectra of the plasma in mixtures of helium with Et_2Zn decomposition products shows that the major emission lines correspond to those of the electronically excited helium and zinc atoms. No emission lines of impurity metals were detected. In Table 3 are given the strongest emission lines of the electronically excited zinc atoms. Assignment of the emission lines of Zn^* and of the energy levels for the lines observed in the emission spectrum was based on data in [23, 24]. No emission lines of electronically excited Zn^{+*} ions were detected, but these ions can be formed in the ground state. The

Table 3. Zn^* lines observed in the emission spectrum of species formed by decomposition of Et_2Zn vapor in electrodeless HF discharge helium plasma

λ_{em}, nm	Assignment	E_{II}, eV[a]
251.581	$4^3P_2 \longleftarrow 7^3D_3$	12.00
256.987	$4^3P_2 \longleftarrow 6^3D_1$	11.83
258.244	$4^3P_1 \longleftarrow 6^3D_2$	11.83
258.249	$4^3P_1 \longleftarrow 6^3D_1$	11.83
260.856	$4^3P_2 \longleftarrow 6^3D_3$	11.83
267.053	$4^3P_0 \longleftarrow 7^3S_1$	11.64
268.416	$4^3P_1 \longleftarrow 7^3S_1$	11.64
271.249	$4^3P_2 \longleftarrow 7^3S_1$	11.64
275.645	$4^3P_0 \longleftarrow 5^3D_1$	11.50
277.087	$4^3P_1 \longleftarrow 5^3D_2$	11.50
277.098	$4^3P_1 \longleftarrow 5^3D_1$	11.50
280.087	$4^3P_2 \longleftarrow 5^3D_3$	11.50
301.835	$4^3P_0 \longleftarrow 6^3S_1$	11.11
303.578	$4^3P_1 \longleftarrow 6^3S_1$	11.11
307.206	$4^3P_2 \longleftarrow 6^3S_1$	11.11
307.590	$4^1S_0 \longleftarrow 4^3P_1$	7.03
328.233	$4^3P_0 \longleftarrow 4^3D_1$	10.78
330.259	$4^3P_1 \longleftarrow 4^3D_2$	10.78
330.294	$4^3P_1 \longleftarrow 4^3D_1$	10.78
334.502	$4^3P_2 \longleftarrow 4^3D_3$	10.78
334.557	$4^3P_2 \longleftarrow 4^3D_2$	10.78
334.593	$4^3P_2 \longleftarrow 4^3D_1$	10.78
462.981	$4^1P_1 \longleftarrow 5^1D_2$	11.47
468.014	$4^3P_0 \longleftarrow 5^3S_1$	9.66
472.216	$4^3P_1 \longleftarrow 5^3S_1$	9.66
481.053	$4^3P_2 \longleftarrow 5^3S_1$	9.66

[a] $E_{II} = 2D + E^*$, where D is the mean energy of bond dissociation in Et_2Zn to form the zinc atom in the ground state; $2D$ = 3.0 eV [22]; E^* is the energy of zinc atom excitation from the ground state to the state from which the given transition is observed in the plasma emission spectrum.

emission spectra also contain very strong emission lines of electronically excited CH^* radicals: a system at 430.0 nm ($A\ ^2\Delta \rightarrow x\ ^2\prod$ transition) and a weaker band at 390.0 nm ($B\ ^2\Sigma \rightarrow x\ ^2\prod$ transition). The most suitable working lines for monitoring deposition of ZnSe films are the Zn^* lines at 307.590, 468.014, 472.216, and 481.053 nm.

When H_2Se vapor is introduced into a plasmochemical reactor in a helium flow, even at room temperature, it actively decomposes, the color of the discharge changes, and a selenium-containing film forms on the support and on reactor walls. The emission spectra were photographed and interpreted with an ISP-30 spectrograph and appropriate photographic plates. Below are the strongest emission lines of electronically excited Se^* atoms:

Table 4. Rate constants of quenching of the emitting levels of the helium atom

Helium level	λ_{em}, nm	Energy of the level, eV	$K_q \times 10^{-8}$, $cm^3\ s^{-1}$	
			Et_2Zn	H_2Se
$4d\ ^3D_{2,1}$	447.148	23.73	16.77 ± 1.38	7.00 ± 0.56
$3p\ ^1D_1$	501.568	23.09	7.00 ± 0.56	3.00 ± 0.24

λ_{em}, nm	Assignment
206.280	$4p^4\ ^1D_2 \longleftarrow 5s\ ^3S_1$
241.350	$4p^4\ ^3P_0 \longleftarrow 5s\ ^3S_1$

Here for both transitions $E_{II} = 2D + E^* = 12.65$ eV; D is the mean energy of bond dissociation in H_2Se to form the Se atom in the ground state; $2D = 6.3$ eV [25, 26]; E^* is the energy of selenium atom excitation from the ground state to the state from which the given transition is observed in the plasma emission spectrum.

We detected no emission lines of electronically excited Se^{+*} ions. Also we detected a weak emission band at about 330.0 nm, tentatively assigned to SeH^*, and a weak emission line of H^* at 486.133 nm. Because the Se^* lines are at the edge of the sensitivity range of the FEU-100 photoelectron multiplier and the SeH^* band at about 330.0 nm is insufficiently strong, it is impossible to work with these lines in the dynamic mode using an MDR-3 monochromator. Thus, monitoring of plasmochemical deposition of ZnSe films from mixtures of He, Et_2Zn, and H_2Se was possible by the lines of only two components: Et_2Zn and He. Monitoring of the intensity of the He^* and Zn^* emission lines showed that the steady state of the discharge is attained within 1.5 min after its switching on. Therefore, all measuremenets were performed after attaining the steady-state mode of the electrodeless HF discharge.

Analysis of the plasma emission spectra shows that introduction of the Et_2Zn or H_2Se vapor into the electrodeless HF discharge helium plasma causes quenching of the emitting levels of the helium atom. We determined the rate constants of quenching of the emitting levels of the He^* atom $4d\ ^3D_{2,1}$ (447.148 nm) and $3p\ ^1P_1$ (501.568 mn) on introducing Et_2Zn and H_2Se vapors into the helium plasma. The results are listed in Table 4. The quenching rate constants K_q of the emitting helium levels were determined from the Stern–Volmer equation $I_0/I = 1 + K_q[Et_2Zn(H_2Se)]/A$, where A is the probability of spontaneous decay of the corresponding helium atomic level; $A = 24.4 \times 10^6\ s^{-1}$ for the level $4d\ ^3D_{2,1}$ and $13.4 \times 10^6\ s^{-1}$ for the level $3p\ ^1P_1$ [26]; [Et_2Zn (H_2Se)] is the concentration of Et_2Zn or H_2Se in the plasmochemical reactor; I_0 is the intensity of the analytical line of the helium atom in the helium atom; and I is the intensity of the same analytical line of the helium atom in the plasma in the presence of Et_2Zn or H_2Se. K_q was determined from the slope of the linear portion of the plot of I_0/I vs. the concentration of the Et_2Zn or H_2Se vapor. Table 4 shows that Et_2Zn quenches the emitting levels of helium more strongly than H_2Se does. Our results correlate with the physicochemical properties of the initial molecules of Et_2Zn and H_2Se such as kinetic diameters of molecules and their ionization potentials (the kinetic diameters of the initial molecules were calculated by the methods of molecular mechanics and by the modified INDO method).

	Et_2Zn	H_2Se
Ionization potential, eV	8.6 [27]	10.0 [25]
Kinetic diameter of the molecule, Å	9.85	5.49

The excited He^* atom under the experimental conditions (P_{He} 82.6 Pa, n_0 2×10^{16}, n_e $1.62 \times 10^{11}\ cm^{-3}$, ε_{av} 6.5 eV, $y_e < 10^{-5}$, where y_e is the degree of helium ionization [$y_e = n_0/n_e$] and ε_{av} is the average electron energy) will be deactivated mainly by the spontaneous decay:

$$He^* \longrightarrow He(1s\ ^1S_0) + h\nu. \qquad (1)$$

The observed quenching will consist in nonelastic interactions of the Et_2Zn and H_2Se molecules introduced into the helium plasma with plasma electrons, responsible also for excitation of helium atoms, decreasing the energy of these electrons:

$$Et_2Zn\ (H_2Se) + e \longrightarrow Products + e. \qquad (2)$$

Process (2) will decrease the fraction of high-energy electrons. Correspondingly will decrease the rate of helium atom excitation from the ground state, the concentration of electronically excited helium atoms, and the intensity of their emission lines. It is known [28] that the larger the kinetic radius of the molecule, the larger the cross section of nonelastic collisions of electrons with this molecule. It is also known that, when a compound with a lower, compared to the inert gas, ionization potential is introduced into an inert gas plasma, the intensities of the emission lines of the electronically excited inert gas atoms decrease. This is due to a decrease in the electron temperature in mixtures of the inert gas and dopant. The decrease in the intensity (at similar concentration of dopants) will be the more pronounced, the lower the ionization

potential of the additive. Thus, both these factors play a role in quenching of the emitting helium levels, and at similar concentration in the gas phase Et_2Zn is a stronger quenching agent than H_2Se.

After elucidating the spectral characteristics of the electrodeless HF discharge plasma, we performed experiments on deposition of ZnSe films from the plasma of mixtures of He with Et_2Zn and H_2Se vapors, with monitoring of the process by the selected analytical lines of the electronically excited He^* and Zn^* atoms. Et_2Zn reacts with H_2Se on the GaAs support as follows:

$$Et_2Zn(g) + H_2Se(g) \xrightarrow{350\times450^\circ C} ZnSe(c) + 2EtH(g), \quad (3)$$

where the indices (g) and (c) refer to the gas phase and the condensate formed on the surface, respectively. Reaction (3) results in deposition of ZnSe(c) on the support and release of ethane into the gas phase. On introduction of the Et_2Zn vapor into the plasmochemical reactor, strong lines of the electronically excited Zn^* atoms appear in the plasma emission spectrum, i.e., Et_2Zn partially decomposes by reactions (4) and (5):

$$Et_2Zn + e \longrightarrow Zn^* + \text{products}, \quad (4)$$

$$Zn^* \longrightarrow Zn^0 + h\nu, \quad (5)$$

where Zn^0 is the zinc atom in the ground ($4s\ ^1S_0$) state. When H_2Se was then fed to the reactor, the intensity of the emission lines of the helium and zinc atoms decreased, and the decrease was the more pronounced, the higher the concentration of H_2Se in the gas phase. Under conditions when $[Et_2Zn]/[H_2Se] \geq 1$ and the He^* and Zn^* lines were observed in the plasma emission spectrum, the photoluminescence spectra of the ZnSe layers deposited on the support were very weak or were not observed at all. Under conditions when $[Et_2Zn]/[H_2Se] < 1$, only the He^* lines were observed in the plasma emission spectrum, the Zn^* lines disappeared, and the photoluminescence spectra of the ZnSe layers deposited on the support were fairly intense. An example of the photoluminescence spectrum of the obtained ZnSe film is shown in the figure (spectrum *1*). It is known that the stoichiometry of ZnSe layers can be monitored by the photoluminescence spectra of films at 77 or 300 K [29]. The spectra of highly perfect films of cubic ZnSe (see figure, spectrum *2*) contain a very strong edge band at 465 nm (300 K) and a weak self-activated band centered at 580 nm. As seen from spectrum *1* in the figure, the photoluminescence spectra of films prepared by direct plasmochemical decomposition of Et_2Zn and

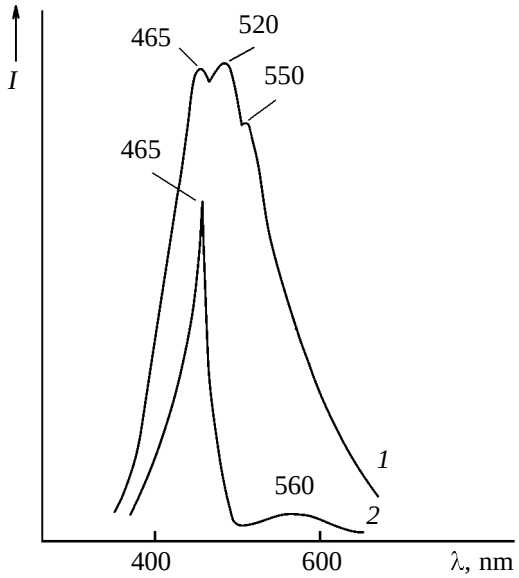

Luminescence spectra of ZnSe samples: (*1*) prepared in the plasma of mixtures of helium with Et_2Zn and H_2Se vapors; (*2*) prepared by thermolysis of the Et_2Zn–H_2Se mixtures.

H_2Se contain a strong edge band at 460 nm, overlapping with a strong self-activated band centered at 520–550 nm. The X-ray phase analysis of the films indicates the growth under these conditions of textured ZnSe(cub) layers with substantial inclusions of the hexagonal phase and with unidentified inclusions. As already noted, under conditions of deposition of ZnSe films, we observed a decrease in the emission lines of Zn^* in the plasma. Therefore, we can assume that quenching of the excited states of the Zn^* atoms is due to the gas-phase reaction of Et_2Zn with H_2Se, resulting in nucleation of ZnSe particles under homogeneous conditions in the gas phase:

$$Et_2Zn(g) + H_2Se(g) \longrightarrow ZnSe(g) + 2EtH(g). \quad (6)$$

Apparently, competition of the ZnSe growth on the support surface [reaction (5)] and in the gas phase [reaction (6)] results in distortion of the single-crystalline structure of the growing layer. Deposition of ZnSe is also accompanied by trapping with the growing surface of active carbon-containing species such as CH, CH_2, etc., generated by decomposition of Et_2Zn in the plasma. The emission spectra of some of these electronically excited species are observed in the plasma. All these factors affect the stoichiometry of the growing layer and ultimately the photoluminescence spectra of the resulting films.

EXPERIMENTAL

Diethylzinc Et_2Zn was prepared by reaction of the Zn–Cu couple with ethyl iodide [30], distilled from the reaction mixture in a vacuum, and purified by

Table 5. Content of metal impurities in Et_2Zn[a]

Element	Content, wt %	Element	Content, wt %
Mn	$< 3\times10^{-4}$	Pb	5×10^{-4}
Al	6×10^{-5}	Sn	5×10^{-4}
Si	4×10^{-4}	Cd	$< 2\times10^{-3}$
Mg	7×10^{-4}	Ge	3×10^{-4}
Fe	$< 9\times10^{-5}$	Cu	7×10^{-4}
Sb	6×10^{-4}		

[a] Analysis for volatiles revealed the presence in diethylzinc of a minor impurity of ethyl iodide (0.1 wt %).

vacuum distillation. The content of metal impurities was determined by spectral analysis. To do this, a sample of Et_2Zn was hydrolyzed with double-distilled water at –30°C in a sealed glass test tube. The resulting zinc hydroxide was dried in a vacuum, with removal of excess water. The residue was calcined at 100°C in an oven. The white powder of zinc oxide was charged into graphite electrodes and burned in a dc arc. The results of analysis of Et_2Zn are listed in Table 5.

Hydrogen selenide was prepared by direct reaction of selenium with hydrogen [31]. The synthesis was performed at 550–600°C in a flow system with condensation of the resulting hydride in a trap cooled with liquid nitrogen. The resulting H_2Se was subjected to thorough multistage purification. Moisture was removed by adsorption, which facilitated removal of dissolved impurities by fractional distillation. Distillation with a low evaporation rate ensured removal of suspended particles. This scheme allowed purification of H_2Se to the following impurity levels: metals 10^{-7} wt %, water 10^{-4} mol %, and hydrocarbons 10^{-6} mol % [31].

The emission properties of the plasma in mixtures of helium with Et_2Zn and H_2Se vapors were studied in a flow-type plasmochemical reactor made of quartz glass. The plasma was generated by electrodeless HF discharge at reduced pressure. The reactor was a tube 50 cm long, 16 mm i.d. Quartz windows were arranged at the ends of the reactor using a special fitting with a sealing gasket. The diameter of the outlet aperture of the quartz windows was 14 mm. To minimize the effect of the reactor walls, helium was passed continuously. The Et_2Zn vapor was fed to the plasmochemical reactor from a special temperature-controlled vaporizer connected to the helium line. The vaporizer temperature was maintained to within ±0.5°C. Hydrogen selenide was fed from a special calibrated vessel equipped with a manometer. The rate of feeding Et_2Zn and H_2Se to the reactor was controlled with rotameters. The concentrations of He, Et_2Zn, and H_2Se were calculated from the measured vapor pressures and gas temperatures on the axis of the plasmochemical reactor. The gas temperature was measured with a thermocouple inserted in a quartz glass capillary (1 mm i.d.).

The ZnSe films were deposited on single-crystalline GaAs [100] and glass supports. The support temperature could be varied within 20–450°C. The GaAs support before deposition was etched in an H_2SO_4–H_2O_2–H_2O mixture, washed with distilled water, dried, and placed in a plasmochemical reactor, which was then evacuated to 1.33 Pa. Then the heater was switched on, a slow flow of H_2Se was fed, and the support was annealed in the H_2Se flow at 450°C for 10 min. Then feeding of H_2Se was stopped, the support was cooled to the temperature of ZnSe deposition, helium was fed, the electrodeless HF discharge was excited, and experiments were started on film deposition or study of plasma emission, with introduction of H_2Se, Et_2Zn, or their mixture. Helium was used as the plasma-forming gas. This choice was governed by the following facts. The first ionization potential of helium, 24.59 eV [32], is considerably higher than those of the other inert gases and, the more so, of Et_2Zn and H_2Se. Metastable states of the helium atom, which are the lower electronically excited states, are located on the energy scale considerably higher than the metastable states of the other inert gas atoms. Since the highest excitation rate is observed for the lower levels and the electron energy distribution function steeply descends at energies higher than that of the first excited level [28], with helium as the plasma-forming gas it is feasible to obtain the electron energy distribution function in which the fraction of high-energy electrons is higher compared to the other inert gases (Ne, Ar, Kr, Xe). One more reason for choosing helium is the fact that the emission spectrum of helium atoms in the range of interest (200–600 nm) contains considerably less lines than the emission spectra of the other inert gases [21]. This fact significantly simplifies treatment of the emission spectra of the electrodeless HF discharge plasma in mixtures of helium with Et_2Zn and H_2Se vapors; also, the probability of overlap of the spectral lines in this case will be lower, i.e., it will be easier to select lines for kinetic studies that would not overlap with the other lines or with emission bands of the plasma. Helium from a cylinder was additionally purified by passing through two series-connected stainless steel traps. The first trap was packed with 4 Å molecular sieves, fraction 0.2–0.5 mm, annealed in a helium flow at 673 K. The second trap was packed

with SKT carbon, fraction 0.3–0.4 mm, annealed in a helium flow at 600 K. The traps were cooled with liquid nitrogen. The helium pressure in the reactor did not exceed 82.6±5.2 Pa; it was monitored with an oil manometer. The plasma emission from the region of location of the support passed through the quartz window and was focused with a lens on the slit of an MDR-3 monochromator with a diffraction grating (1200 lines per millimeter), equipped with an FEP-3 recorder, or on the slit of an ISP-30 spectrograph. In the first case, the radiation was detected with an FEU-100 photoelectron multiplier (sensitivity range 220–800 nm). The scan scale of the MDR-3 drum was calibrated with a standard mercury source (PRK-4 lamp) and with the helium discharge spectrum. The plasma emission spectra were also photographed with an ISP-30 spectrograph (working range 200–600 nm). The iron arc spectrum, used as reference in interpretation of the plasma emission spectra, was excited with an IVS-29 generator. The spectra were photographed with ES-type and orthonormal spectrographic plates. A Hartmann diaphragm was put on the slit of the ISP-30 spectrograph when photographing the spectra. The optical devices were tuned with an OKG-13 helium–neon laser.

To determine the parameters of the electrodeless HF discharge helium plasma, we took a plasmochemical reactor of identical size and introduced two mobile cylindrical tungsten probes into the working volume in the region of the center of the ten-turn excitation solenoid. The probes were 100 μm in diameter, the length of the glass-free part was 2.5 mm, and the distance between the probes was 2 mm. The mobile probes were designed on the basis of a Teflon stopcock. Using these probes, we measured the current–voltage characteristic of the discharge on the axis of the plasmochemical reactor. From this characteristic we determined graphically the electron temperature T_e. The electron concentration was determined from the saturation ion current [33].

The phase composition of ZnSe films was studied with a DRON-3M diffractometer using graphite-monochromated CuK radiation on diffracted beam. The films were also studied by electron diffraction in the reflection mode (ER-100). The photoluminescence spectra of films were taken in a special cell at 300 K. The ZnSe luminescence was excited with an LGI-21 nitrogen laser (λ 337 nm, incident beam power 0.3 mW cm^{-2}, beam diameter 3 mm).

ACKNOWLEDGMENTS

The study was financially supported by the Russian Foundation for Basic Research (project nos. 95-03-08273a and 96-15-97455).

REFERENCES

1. Gribov, B.G., Domrachev, G.A., Zhuk, B.V., Kaverin, B.S., Kozyrkin, B.I., Mel'nikov, V.V., and Suvorova, O.N., *Osazhdenie plenok i pokrytii razlozheniem metalloorganicheskikh soedinenii* (Deposition of Films and Coatings by Decomposition of Organometallic Compounds), Razuvaev, G.A., Ed., Moscow: Nauka, 1981.
2. Zhuk, B.V., *Usp. Khim.*, 1985, vol. 54, no. 8, pp. 1312–1334.
3. Bregadze, V.I., Golubinskaya, L.M., and Usyatinskii, A.Ya., *Metalloorg. Khim.*, 1988, vol. 1, no. 3, pp. 517–533.
4. Segui, Y., Carrere, F., and Bui, A., *Thin Solid Films*, 1982, vol. 92, no. 4, pp. 303–307.
5. Carrere, F., Segui, Y., and Moret, B., *Int. Chim.*, 1983, no. 234, pp. 107–109.
6. Pande, K.P. and Seabaugh, A.C., *J. Electrochem. Soc.*, 1984, vol. 131, no. 6, pp. 1357–1359.
7. Dobrynin, A.V., Zorina, E.N., Popova, T.O., Neustroev, S.A., and Sokolov, E.B., *Khim. Vys. Energ.*, 1979, vol. 13, no. 2, pp. 161–164.
8. Sato, M., *J. Appl. Phys.*, 1995, vol. 78, no. 3, pp. 2123–2125.
9. Sato, M., *Appl. Phys. Lett.*, 1996, vol. 68, no. 7, pp. 935–937.
10. Tokeda, T., Wakahara, A., Noda, S., and Sosaki, A., *J. Cryst. Growth*, 1997, vol. 173, nos. 3–4, pp. 237–243.
11. Wang, J., Zhu, Z., Park, K.T., Higara, K., and Yao, T., *J. Electron. Mater.*, 1997, vol. 26, no. 3, pp. 232–236.
12. Yasui, K., Iizuka, K., Harada, T., and Akahane, T., *Jpn. J. Appl. Phys., Part 1*, 1997, vol. 36, no. 7B, pp. 4953–4958.
13. Yasuda, T., Hata, K., Mizuta, M., and Kukimoto, H., *J. Cryst. Growth*, 1989, vol. 96, no. 4, pp. 979–981.
14. Matumoto, T., Chen, H., Kasabitaki, N., Maekama, Y., and Aozasa, M., *Mem. Fac. Eng. Osaka City Univ.*, 1993, no. 34, pp. 25–32.
15. Fujiwa, H., Nabeta, T., Kiryu, H., and Shimizu, I., *Jpn. J. Appl. Phys., Part 1*, 1994, vol. 33, no. 7B, pp. 4381–4384.
16. Yamamoto, K. and Taguchi, T., *Mem. Fac. Eng. Yamaguchi Univ.*, 1995, vol. 45, no. 2, pp. 311–335.
17. Taudt, W., Wachtendorf, B., Samerlander, F., Hamaden, H., Lampe, S., and Heuken, M., *J. Electron. Mater.*, 1995, vol. 24, no. 11, pp. 1671–1675.
18. Morimoto, K., *J. Cryst. Growth*, 1996, vol. 159, nos. 1–4, pp. 317–320.
19. Taudt, W., Hardt, A., Lampe, S., Hamaden, H., and

Heuken, M., *J. Cryst. Growth*, 1997, vol. 170, nos. 1–4, pp. 491–496.

20. Striganov, A.R. and Odintsova, G.A., *Tablitsy spektral'nykh linii atomov i ionov: Spravochnik* (Tables of Spectral Lines of Atoms and Ions: Handbook), Moscow: Energoizdat, 1982.
21. Zaidel', A.N., Prokof'ev, V.K., Raiskii, S.M., Slavnyi, V.A., and Shreider, E.Ya., *Tablitsy spektral'nykh linii: Spravochnik* (Tables of Spectral Lines: Handbook), Moscow: Nauka, 1977.
22. Tel'noi, V.I. and Rabinovich, I.B., *Usp. Khim.*, 1980, vol. 49, no. 7, pp. 1137–1173.
23. Hetzlier, C.W., Boreman, R.W., and Burns, K., *Phys. Rev.*, 1935, vol. 48, no. 5, pp. 656–659.
24. Moore, C.E., in *Atomic Energy Levels, Circular of the National Bureau of Standards*, 1952, no. L67, vol. 2.
25. Balkis, T., Gaines, A.F., Ozgen, G., Ozgen, I.T., and Flowers, M.C., *J. Chem. Soc., Faraday Trans. 2*, 1976, vol. 72, no. 3, pp. 524–527.
26. *Spetsial'nyi fizicheskii praktikum* (Special Practical Course of Physics), Moscow: Mosk. Gos. Univ., 1977, part 2, p. 180.
27. Creber, D.K. and Bancroft, G.M., *Inorg. Chem.*, 1980, vol. 19, no. 3, pp. 643–648.
28. Slovetskii, D.I., *Mekhanizmy khimicheskikh reaktsii v neravnovesnoi plazme* (Mechanisms of Chemical Reactions in Nonequilibrium Plasma), Moscow: Nauka, 1980.
29. Razov, E.N., Korotysheva, E.E., Zhuk, B.V., Kaverin, B.S., and Rybnikov, V.V., *Metalloorg. Khim.*, 1988, vol. 1, no. 3, pp. 586–591.
30. Sheverdina, N.I. and Kocheshkov, K.A., *Metody elementoorganicheskoi khimii. Tsink. Kadmii* (Methods of Organometallic Chemistry. Zinc. Cadmium), Moscow: Nauka, 1974, p. 14.
31. Devyatykh, G.G. and Churbanov, M.F., *Vysokochistye khal'kogenidy* (High-Purity Chalcogenides), Nizhny Novgorod: Nizhegorod. Univ., 1997, pp. 186–189.
32. Gurvich, L.V., Karachevtsev, G.V., Kondrat'ev, V.N., Lebedev, Yu.A., Medvedev, V.A., Potapov, V.K., and Khoddeev, Yu.S., *Energii razryva khimicheskikh svyazei. Potentsialy ionizatsii i srodstvo k elektronu* (Dissociation Energies of Chemical Bonds. Ionization Potentials and Electron Affinity), Moscow: Nauka, 1974.
33. Kozlov, O.V., *Elektricheskii zond v plazme* (Electric Probe in Plasma), Moscow: Atomizdat, 1969, pp. 90, 190.